

Differential Expression of *PKD2*-Associated Genes in Autosomal Dominant Polycystic Kidney Disease

Yeon Joo Yook[†], Yu Mi Woo[†], Moon Hee Yang, Je Yeong Ko, Bo Hye Kim, Eun Ji Lee, Eun Sun Chang, Min Joo Lee, Sunyoung Lee and Jong Hoon Park*

Department of Biological Science, Sookmyung Women's University, Seoul 140-742, Korea

Abstract

Autosomal dominant polycystic kidney disease (ADPKD) is characterized by formation of multiple fluid-filled cysts that expand over time and destroy renal architecture. The proteins encoded by the *PKD1* and *PKD2* genes, mutations in which account for nearly all cases of ADPKD, may help guard against cystogenesis. Previously developed mouse models of *PKD1* and *PKD2* demonstrated an embryonic lethal phenotype and massive cyst formation in the kidney, indicating that *PKD1* and *PKD2* probably play important roles during normal renal tubular development. However, their precise role in development and the cellular mechanisms of cyst formation induced by *PKD1* and *PKD2* mutations are not fully understood. To address this question, we presently created *Pkd2* knockout and *PKD2* transgenic mouse embryo fibroblasts. We used a mouse oligonucleotide microarray to identify messenger RNAs whose expression was altered by the overexpression of the *PKD2* or knockout of the *Pkd2*. The majority of identified mutations was involved in critical biological processes, such as metabolism, transcription, cell adhesion, cell cycle, and signal transduction. Herein, we confirmed differential expressions of several genes including aquaporin-1, according to different *PKD2* expression levels in ADPKD mouse models, through microarray analysis. These data may be helpful in *PKD2*-related mechanisms of ADPKD pathogenesis.

Keywords: cystogenesis, MEF cells, microarray, *PKD2*, polycystic kidney disease

Introduction

Autosomal dominant polycystic kidney disease (ADPKD) is a common monogenetic disorder, affecting as many as 1 in 500 people in the general population. The disease is characterized by the formation of multiple fluid-filled renal cysts that expand over time and destroy the architecture of the kidney. Five percent of all cases of chronic renal failure are due to ADPKD, and approximately 50% of ADPKD patients will develop end-stage renal disease by the time they are 60 years of age [1].

In the early stages of ADPKD, numerous cysts begin to enlarge from many segments of the kidney. Later, the enlarged regions disassociate from the original nephron to form the actual cysts, which continue to enlarge due to proliferation of epithelial cells and fluid secretion into the cyst lumen. Progressive renal cyst formation and enlargement result in a loss of renal function and hypertension and culminate in renal failure. It is generally believed that cysts enlarge by means of abnormal cell growth, forming what is essentially a fluid-filled tumor that fills by transepithelial fluid secretion. Cyst enlargement may then lead to extracellular matrix remodeling, interstitial fibrosis, a general inflammatory response, and disruption of the normal renal parenchyma, which then interfere with glomerular filtration and vascular blood flow, giving rise to cell death by apoptosis and ultimately renal failure [2].

Many studies have indicated that most cases of ADPKD are accounted for by mutations in the *PKD1* and *PKD2* genes, encoding the transmembrane protein polycystin-1 (PC1) and polycystin-2 (PC2), respectively. Mice with targeted mutations in the *PKD1* or *PKD2* genes develop cystic kidneys during embryogenesis, and ADPKD in humans is associated with mutations in the *PKD1* or *PKD2* genes [3, 4]. In addition, the product of the *PKD1* gene, PC1, has been implicated in a variety of pathways tied to proliferation, including G-protein signaling and the Wnt, activator protein 1 (AP-1), and Janus kinase-signal transducers and activators of transcription cascades [5, 6]. Moreover, depletion of PC1 has been shown to increase cell growth, whereas its overexpression slows cell growth, indicating that PC1 may negatively regulate cell proliferation [7, 8]. PC2, the protein product of *PKD2*, has also been implicated in cell cycle regulation via its calcium channel activity and stimulation of AP-1 [9, 10]; however, there has been little direct evidence tying PC2 to this process.

[†]These authors contributed equally to this work.

*Corresponding author: E-mail parkjh@sookmyung.ac.kr
Tel +82-2-710-9414, Fax +82-2-2077-7322

Received 30 January 2012, Revised 15 February 2012,
Accepted 16 February 2012

Here, we created a number of related cell lines that varied in their expression of PK2. We describe studies designed to identify target genes under the control of the *PKD2* using *Pkd2* knockout (KO) and *PKD2* transgenic (TG) mouse embryo fibroblasts (MEFs). We used a mouse 30 K whole gene oligonucleotide microarray to identify messenger RNAs whose expression was altered by the overexpression of the *PKD2* or KO of the *Pkd2* in MEF cells.

Methods

Establishment of MEF derived from wild-type and *PKD2* mutation embryos

MEF were acquired from *PKD2* TG embryos or *Pkd2* KO embryos during development (13.5 days) [11]. Heads and limes were removed from embryos. The remaining embryonic tissues were minced and dispersed in 0.05% trypsin prior to incubation at 37°C for 15 min. Cells were plated in Dulbecco's Modified Eagle's Medium of Defined Minimal Essential medium (Welgene Biotech, Taipei, Taiwan) supplemented with 10% fetal bovine serum (Welgene Biotech) and were cultured at 37°C in an atmosphere of 5% CO₂ until confluent growth was achieved. MEF cells were frozen as stocks at the second passage and were used for the subsequent studies at the third passage.

Microrray hybridization and data analysis

Total RNA was prepared using a commercial kit (Qiagen, Valencia, CA, USA) according to the manufacturer's instructions. Gene expression profiles were obtained using the CodeLink Uniset Mouse Expression Bioarray (Amersham, Buckinghamshire, UK). The 30,000 gene probes contained in the bioarray allows the detection of differences in gene expression as low as 1.3-fold with 95% confidence. Ten micrograms of total RNA was amplified, and labeled cDNA was produced. Biotin-labeled cDNA was hybridized to the array overnight in a shaking incubator at 37°C, and excess target sequences were washed away using a series of saline sodium citrate washes. The array was stained by treatment with streptavidin-Alexafluor 647 (Molecular Probes, Eugene, OR, USA), the excess was washed away, and the array was scanned at an excitation wavelength of 632 nm using a GenePix scanner (Molecular Devices, Sunnyvale, CA, USA). The resulting image was quantified, and the intensity of each spot was divided by the median spot intensity to provide a scaled and comparable number across multiple arrays.

DNA microarray scanning and analysis

Microarrays were scanned using an Arraywax scanner (Applied Precision, Seattle, WA, USA), analyzed using ImaGene version 5.1 software (Biodiscovery, Segundo, CA, USA), and normalized using Genesight version 3.2 software (Biodiscovery). Normalization was performed by subtracting the means of all genes. The data normalized by Genesight were compared using an M/A plot. Genes differentially expressed were identified by intensity differences, after subtracting the background intensity. Genes showing expression changes of at least 2-fold were selected, and these selected genes were clustered by the hierarchical method.

Clustering algorithm

The normalized log ratio corresponding to each time point was exported to the software for clustering algorithm. Acuity version 3.1 (Molecular Devices) was used for the 'gene shaving' algorithm. To estimate the number of clusters in a dataset, the 'Gap Statistics' attribute of the Acuity software package was used. The cluster number, estimated by gap statistics, was used for an input parameter in gene shaving. After gene shaving, a single linkage was used for hierarchical clustering.

Semi-quantitative and real-time RT-PCR

Total RNA was prepared using a commercial kit (Qiagen) according to the manufacturer's instructions. Single-strand cDNA was synthesized by incubating 5 µg total RNA with 200 units AMV, 100 nM oligo(dT)₁₂₋₁₈, 1 mM dNTP mixture, and 40 units RNase inhibitor at 42°C for 1 h in a final volume of 25 µL. The reaction was terminated by incubation at 70°C for 15 min. The initial amount of mRNA and reaction conditions were optimized to obtain linearity for mouse *18s rRNA*. For semi-quantitative reverse transcription (RT)-PCR, the used primers were: human *PKD2*, forward 5'-CGTGCCCCAGCCCAGTC-3' and reverse 5'-TTCCAGTACAGCCCATCCAATAAG-3'; mouse *Pkd2*, forward 5'-TGCGAGGGCTGCGAGGTC-3' and reverse 5'-TGTCAGCTTGCCTGTGGTTGC-3'; mouse *18s rRNA*, forward 5'-GTAACCCGTTGCACCCCATT-3' and reverse 5'-CCATCCAATCGGTAGTAGCG-3'. RT-PCR cycling conditions were as follows: 10 min at 95°C, 25 cycles of 50 s at 94°C, 50 s at 57°C, 50 s at 72°C, and 5 min at 72°C. The amplified products were separated on a 1% agarose gel. For real-time PCR, the used primers were: mouse *β-actin*, (forward 5'-GACGATGCTCCCGGGCTGTATTC-3' and reverse 5'-TCTCTTGCTCTGGCCTCGTCACC-3') used as a positive control; mouse peroxisome proliferator-activated receptor γ (*PPAR-γ*),

forward 5'-TCTTAACTGCCGGATCCACAAAAA-3' and reverse 5'-ATCTCCGCCAACAGCTTCTCCTTC-3'; mouse protein kinase α (*PKC α*), forward 5'-GGGCAGCCTCCGTTTGATGGT-3' and reverse 5'-CGCTTGGCAGGGTGT TTGGTC-3'; mouse *Wnt4*, forward 5'-GCCATCGAGGAG TGCCAATACC-3' and reverse 5'-GGCCACACCTGCTGA AGAGATG-3'; mouse integrin $\alpha 4$ (*ITG $\alpha 4$*), forward 5'-GTAGCCCCAGTGGAGAGCCTTGTG-3' and reverse 5'-ATGCCAGTGGGGAGTTTGTATCG-3'; mouse *IL6ST*, forward 5'-TGAATCGGACCCACTTGAGAGG-3' and reverse 5'-CAGGAGCGGCTTGTGAGGTA-3'; mouse aquaporin 1 (*AQP1*), forward 5'-GGAGGCGCCGAGACTTAGGT-3' and reverse 5'-GCGGGTGAGCACAGCAGAGC-3'; mouse transforming growth factor- $\beta 2$ (*TGF- $\beta 2$*), forward 5'-TCATCCCGAATAAAAGCGAAGAGC-3' and reverse 5'-AGGGCAACAACATTAGCAGGAGAT-3'. Real-time RT-PCR was performed using the real-time SensiMixPlus SYBR kit as described by the manufacturer's instructions (Quantance, London, UK).

Western blot analysis

Proteins were extracted using radio-immunoprecipitation assay buffer in MEF cells. Proteins were separated by 12% sodium dodecyl sulfate-polyacrylamide gel electrophoresis and were transferred to a polyvinylidene fluoride membrane (Millipore, Bellerica, MA, USA). Membranes were blocked with 5% non-fat dry milk and were incubated with various antibodies. Antibodies to PC2 (anti-human and anti-mouse) and AQP1 were obtained from Santa Cruz Biotechnology (Santa Cruz, CA, USA). Antibodies to β -actin were obtained from Sigma-Aldrich (St. Louis, MO, USA). Anti-Wnt4 was obtained from R&D Systems (Minneapolis, MN, USA). Each membrane was washed with phosphate-buffered saline-Tween, and immunocomplexes were detected by enhanced chemiluminescence (Amersham).

Results

Confirmation of *PKD2* expression in *Pkd2* KO and *PKD2* TG MEFs

Mouse *Pkd2* mRNA was revealed in KO wild-type (KOWT) MEF cells but not in KO MEF cells. Also, *Pkd2* mRNA was expressed in TG wild-type (TGWT) MEF cells and *PKD2* TG MEF cells. Human *PKD2* mRNA was only expressed in *PKD2* TG MEF cells obtained from *PKD2* TG embryos following injection of the human *PKD2* transgene (Fig. 1A). Consistently, the expression level of polycystin-2 was lower in KO MEFs than KOWT MEFs as well as higher in TG MEFs than TGWT MEFs (Fig. 1B).

Microarray gene expression analysis

We used a mouse 30 K whole gene oligonucleotide microarray to identify mRNAs whose expression was altered by the *Pkd2* KO and *PKD2* TG MEF cells. The normalized log ratios corresponding to each time point were exported to the software for clustering algorithm. We used Axon's Acuity 3.1 (Axon Instruments, Union City, CA, USA) for using the 'gene shaving' algorithm. To estimate the number of clusters in a dataset, we used 'Gap Statistics' in Acuity 3.1. The cluster number estimated by gap statistics was used for an input parameter in gene shaving. After gene shaving, we used a single linkage hierarchical clustering. The single linkage hierarchical clustering method divides 8 'gene shaving' clusters (Fig. 2). The majority of genes whose expression was appreciably altered encoded proteins involved in critical biological processes, such as metabolism, transcription, cell adhesion, cell cycle, and signal transcription. Forty-five genes whose expression was changed by 2-fold or greater were identified (Table 1).

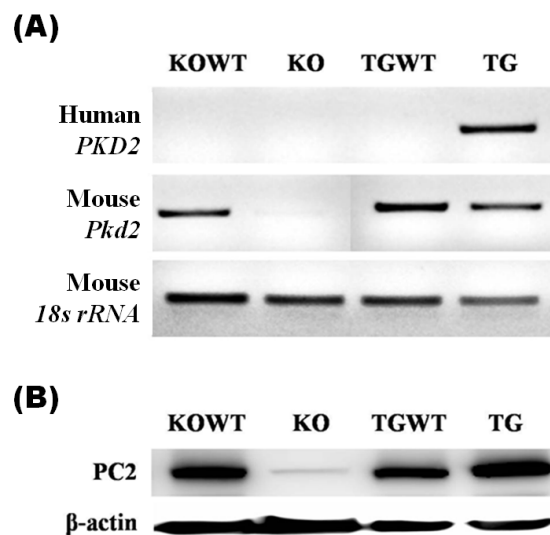


Fig. 1. Establishment of *Pkd2* KO and *PKD2* TG MEFs. (A) Semi-quantitative reverse transcription-PCR analysis of *Pkd2* gene in *Pkd2* KO and *PKD2* TG MEF cells. Human- or mouse-specific *PKD2* primer sets were used. *18s rRNA* was used as a loading control. (B) Western blot analysis of polycystin 2 (PC2) expression in *Pkd2* KO and *PKD2* TG MEF cells. MEFs, mouse embryo fibroblasts; KO, knockout (MEF); TG, transgenic (MEF); KOWT, knockout wild-type (MEF); TGWT, transgenic wild-type (MEF).

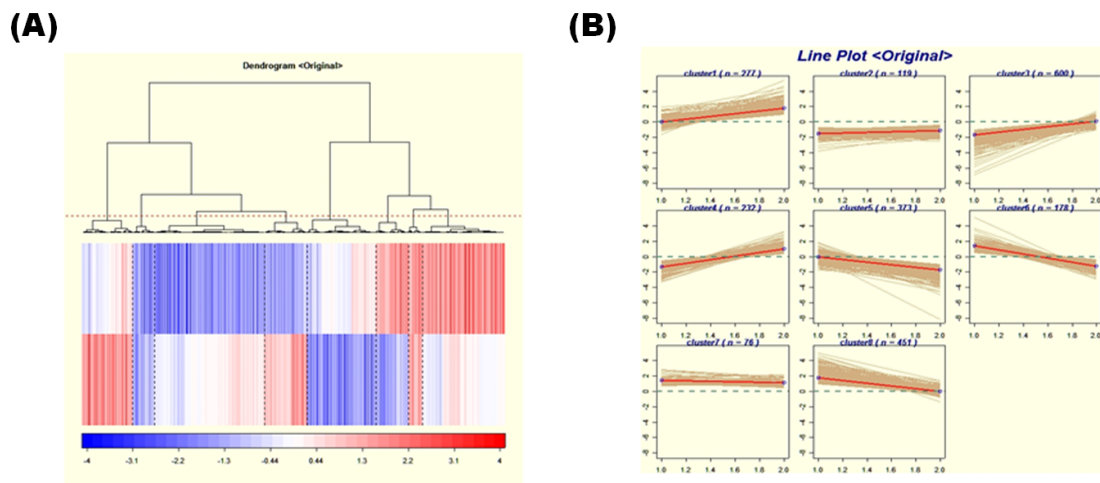


Fig. 2. Clustering of gene expression patterns in *Pkd2* mutant MEF cell lines. We performed clustering analysis microarray data between KO set ratio data and TG set ratio data using the graphical user interface (GUI) system. (A) Gene expression profiles of 2,306 probe sets distributed in a dendrogram, (B) Line plots of each cluster. KO set, ratio between KO MEF and KOWT MEF; TG set, ratio between TG MEF and TGWT MEF. MEFs, mouse embryo fibroblasts; KO, knockout (MEF); TG, transgenic (MEF); KOWT, knockout wild-type (MEF); TGWT, transgenic wild-type (MEF).

Verification of candidate genes by quantitative RT-PCR and immunoblot analysis

To verify the results obtained by cDNA microarray analysis, expression patterns for selected genes were confirmed at the RNA and protein levels. We selected seven genes among the 45 genes (Fig. 3A). As result of real-time RT-PCR, the expression patterns of *PKCa*, *ITGa4*, and *AQP1* were identical to microarray analysis in *Pkd2* KO MEF cells (Fig. 3B). In contrast, 6 genes, except for *TGF- β 2*, were identically expressed in *PKD2* TG MEF cells (Fig. 3C). Especially, the *AQP1* gene may be significantly regulated by differential *Pkd2* gene expression level. Furthermore, to confirm the AQP1 protein expression level, western blot analysis was performed using MEF cells as well as kidney tissues obtained from *Pkd2* KO (or heterozygote) and *PKD2* TG mice. As result, AQP1 protein level was consistent with mRNA levels in both MEFs and tissues (Fig. 4).

Discussion

Although remarkable progress toward understanding the genetics and pathophysiology of ADPKD has been made to date, it is still unclear how mutations in disease-causing genes trigger cystogenesis and what important role other molecules play in the cystic phenotype [12]. Our aim here was to identify genes associated with the cystic phenotype using *Pkd2* KO and *PKD2* TG MEF cells. In a previous study, overexpression of human *PKD2* led to anomalies in tubular function, due to abnormalities in

tubule morphogenesis [13]. Similar findings have been made for the *PKD1* gene. For this gene, gain/loss of function and haploinsufficiency leads to cystogenesis, with the severity of the phenotype being related to the level of imbalance. More severe phenotypes are seen for gain and loss of function than for haploinsufficiency [4]. In the present study, the association between cystogenesis and the loss or gain of *PKD2* supports the idea that PC2 functions through *Pkd2* mutant MEF cells.

Presently, we found Wnt4 to be up-regulated in *Pkd2* KO MEF cells and down-regulated in *PKD2* TG MEF cells. Wnt4, a member of the Wnt family of lipid-modified secreted glycoproteins, plays central roles in the initial stages of the tubulogenic program. Wnt4 is expressed in the pretubular aggregate, as one of the first molecular responses to inductive signaling mediated by ureteric epithelium [14].

AQP1 was observed to be up-regulated in both *Pkd2* KO and *PKD2* TG MEF cells. AQP1 is a channel-forming integral membrane protein found in erythrocytes and water-transporting tissues, including the kidney, where it is localized to the proximal tubules and thin descending limbs of Henle's loop. The selective expression pattern of AQP1 in human nephrogenesis suggests that proximal tubules and thin descending limbs become permeable to water early in development. A predominantly apical expression of AQP1 is found during a critical period of the nephrogenesis, during formation of the proximal tubule, as well as in the early stage of ADPKD; in normal tubules, distribution is both apical and basolateral [15]. Another interesting defect in urine-concen-

trating ability was described in the *Aqp1* knockout mouse. Although these mice were grossly normal in terms of survival and appearance, they were vulnerable to water deprivation and became severely dehydrated. These results suggest that AQP1 is required for the formation of concentrated urine [16].

We have found PKC- α and Bcl-2 associated transcription factor to be down-regulated in *Pkd2* KO MEF cells and up-regulated in *PKD2* TG MEF cells. Recent observations in animal models of PKD have implicated apoptosis in its pathogenesis. PKC- and Erk-dependent pathways are critical components of the cell survival by sup-

pressing the apoptosis [17]. We also have demonstrated the role for *PKD2* in cellular adhesion processes. In this study, *ITG α 4* was up-regulated in *Pkd2* KO MEF cells and down-regulated in *PKD2* TG MEF cells. It suggests that adhesion molecule such as *ITG α 4* may be associated with *PKD2* mutation-related pathogenesis.

In conclusion, by using the cDNA microarray technique, we have found several candidate genes that may be involved in cystogenesis: PKC α , *ITG α 4* and AQP1. These genes were affected by *PKD2* expression and may be related to cyst formation of kidney together with the *PKD2* gene.

Table 1. Genes deregulated by differential *Pkd2* expression

GenBank Accession no.	Definition	Fold change	
		KO	TG
Proliferation			
NM_008275,2	Homeo box D13	1,00	0,38
NM_008783,1	Pre B-cell leukemia transcription factor 1	0,38	1,93
NM_011245,2	RAS protein-specific guanine nucleotide releasing factor 1	3,64	1,36
NM_009367,1	Transforming growth factor, beta 2	0,49	1,22
NM_013693,1	Tumor necrosis factor	0,30	0,27
Apoptosis			
NM_001025393,1	BCL2-associated transcription factor 1	0,36	1,23
NM_007465,1	Baculoviral IAP repeat-containing 2	1,32	0,20
NM_001038658,1	FAS apoptotic inhibitory molecule 2	0,81	0,44
NM_011563,2	Peroxiredoxin 2	0,48	0,85
NM_011101,1	Protein kinase C, alpha	0,21	1,49
NM_011609,2	Tumor necrosis factor receptor superfamily, member 1a	0,24	0,93
PPAR gamma			
NM_011146,1	Peroxisome proliferator activated receptor gamma	0,37	1,64
NM_008904,1	Peroxisome proliferative activated receptor, gamma, coactivator 1 alpha	0,59	0,49
NM_133249,2	Peroxisome proliferative activated receptor, gamma, coactivator 1 beta	0,20	0,37
Wnt			
NM_011718,1	Wingless related MMTV integration site 10b	0,31	0,90
NM_008058,1	Frizzled homolog 8 (drosophila)	0,43	1,09
NM_009523,1	Wingless related MMTV integration site 4	5,21	0,72
NM_009331,2	Transcription factor, T-cell specific	2,99	0,74
Chemokine			
NM_008176,1	Chemokine (C-X-C motif) ligand 1	3,97	1,08
NM_021704,2	Chemokine (C-X-C motif) ligand 12	0,44	1,05
NM_009911,2	Chemokine (C-X-C motif) receptor 4	2,66	0,55
NM_009140,1	Chemokine (C-X-C motif) ligand 2	2,75	1,27
Aquaporin			
NM_007472,1	Aquaporin 1	1,43	2,27
NM_016689,2	Aquaporin 3	1,23	2,01
Interleukin			
NM_010560,2	Interleukin 6 signal transducer	0,31	1,61
NM_008353,1	Interleukin 12 receptor, beta1	2,20	1,89
NM_008356,1	Interleukin 13 receptor, alpha2	4,03	0,85
NM_134437,1	Interleukin 17 receptor D	2,28	1,06
NM_133193,1	Interleukin 1 receptor-like 2	2,41	0,85
Integrin			
NM_010576,3	Integrin alpha 4	2,55	0,48

KO, knockout; TG, transgenic.

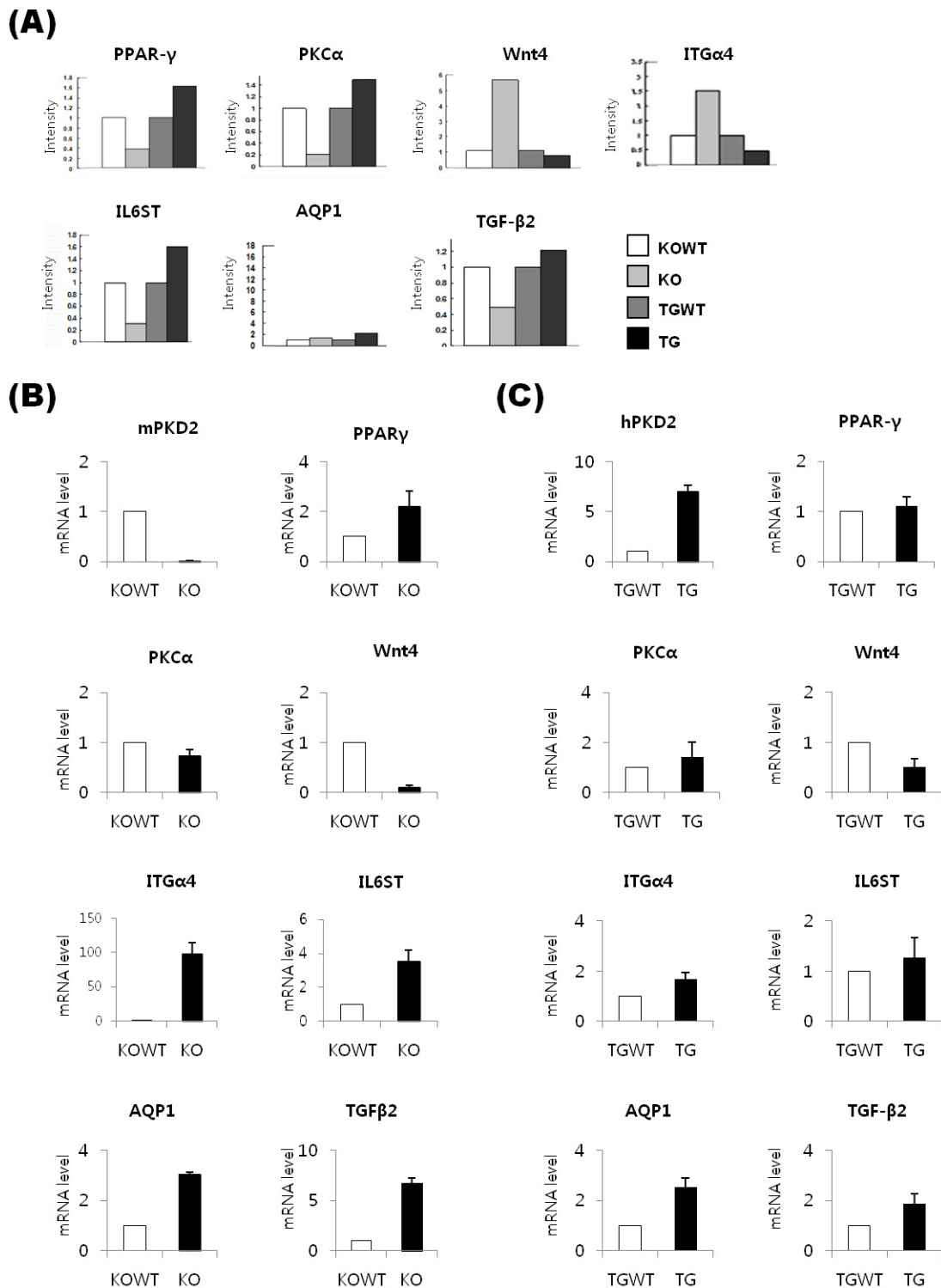


Fig. 3. Expression verification of candidate genes at the mRNA level. (A) Microarray data for selective genes including *PPAR γ* , *PKC α* , *Wnt4*, *ITG α 4*, *IL6ST*, *AQP1*, and *TGF- β 2*. (B, C) Real-time reverse transcription-PCR analysis of gene expression for selective genes in *Pkd2* KO and *Pkd2* TG MEF cells. *β -actin* primer was used as the internal control. The experiment was performed in triplicate. *PPAR- γ* , peroxisome proliferator-activated receptor γ ; *PKC α* , protein kinase α ; *ITG α 4*, integrin α 4; *AQP1*, aquaporin 1; *TGF- β 2*, transforming growth factor- β 2; KO, knockout; TG, transgenic; MEF, mouse embryo fibroblasts; KOWT, knockout wild-type (MEF); TGWT, transgenic wild-type (MEF).

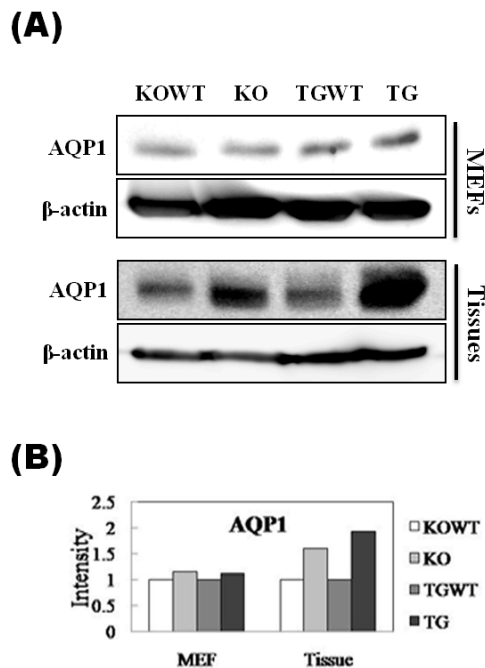


Fig. 4. Expression verification of AQP1 at the protein level. (A) Western blot analysis of AQP1 in MEFs and kidney tissues derived from *Pkd2* KO (or heterozygote) and *PKD2* TG mice. *PKD2* TG and TGWT mice: 18 mo; *Pkd2* heterozygote and KOWT mice: 12 mo. Anti- β -actin was used as the internal control. (B) For quantification of western blot, Multigauge software (Fuji Film) was used. AQP1, aquaporin 1; MEF, mouse embryo fibroblasts; KO, knockout; TG, transgenic; KOWT, knockout wild-type (MEF); TGWT, transgenic wild-type (MEF).

Acknowledgments

This work was supported by a Sookmyung Women's University Research Grant (2010).

References

- Grimm DH, Karihaloo A, Cai Y, Somlo S, Cantley LG, Caplan MJ. Polycystin-2 regulates proliferation and branching morphogenesis in kidney epithelial cells. *J Biol Chem* 2006;281:137-144.
- Wilson PD, Falkenstein D. The pathology of human renal cystic disease. *Curr Top Pathol* 1995;88:1-50.
- Kim K, Drummond I, Ibraghimov-Beskrovnya O, Klinger K, Arnaout MA. Polycystin 1 is required for the structural integrity of blood vessels. *Proc Natl Acad Sci U S A* 2000;97:1731-1736.
- Wu G, D'Agati V, Cai Y, Markowitz G, Park JH, Reynolds

- DM, *et al.* Somatic inactivation of *Pkd2* results in polycystic kidney disease. *Cell* 1998;93:177-188.
- Arnould T, Kim E, Tsiokas L, Jochimsen F, Gruning W, Chang JD, *et al.* The polycystic kidney disease 1 gene product mediates protein kinase C alpha-dependent and c-Jun N-terminal kinase-dependent activation of the transcription factor AP-1. *J Biol Chem* 1998;273:6013-6018.
- Parnell SC, Magenheimer BS, Maser RL, Zien CA, Frischauf AM, Calvet JP. Polycystin-1 activation of c-Jun N-terminal kinase and AP-1 is mediated by heterotrimeric G proteins. *J Biol Chem* 2002;277:19566-19572.
- Boletta A, Qian F, Onuchic LF, Bhunia AK, Phakdeekitcharoen B, Hanaoka K, *et al.* Polycystin-1, the gene product of PKD1, induces resistance to apoptosis and spontaneous tubulogenesis in MDCK cells. *Mol Cell* 2000;6:1267-1273.
- Kim H, Bae Y, Jeong W, Ahn C, Kang S. Depletion of PKD1 by an antisense oligodeoxynucleotide induces premature G1/S-phase transition. *Eur J Hum Genet* 2004;12:433-440.
- Gallagher AR, Cedzich A, Gretz N, Somlo S, Witzgall R. The polycystic kidney disease protein PKD2 interacts with Hax-1, a protein associated with the actin cytoskeleton. *Proc Natl Acad Sci U S A* 2000;97:4017-4022.
- Luo Y, Vassilev PM, Li X, Kawanabe Y, Zhou J. Native polycystin 2 functions as a plasma membrane Ca²⁺-permeable cation channel in renal epithelia. *Mol Cell Biol* 2003;23:2600-2607.
- Park EY, Sung YH, Yang MH, Noh JY, Park SY, Lee TY, *et al.* Cyst formation in kidney via B-Raf signaling in the PKD2 transgenic mice. *J Biol Chem* 2009;284:7214-7222.
- Husson H, Manavalan P, Akmaev VR, Russo RJ, Cook B, Richards B, *et al.* New insights into ADPKD molecular pathways using combination of SAGE and microarray technologies. *Genomics* 2004;84:497-510.
- Burtey S, Riera M, Ribe E, Pennekamp P, Passage E, Rance R, *et al.* Overexpression of PKD2 in the mouse is associated with renal tubulopathy. *Nephrol Dial Transplant* 2008;23:1157-1165.
- Park JS, Valerius MT, McMahon AP. Wnt/beta-catenin signaling regulates nephron induction during mouse kidney development. *Development* 2007;134:2533-2539.
- Devuyst O, Burrow CR, Smith BL, Agre P, Knepper MA, Wilson PD. Expression of aquaporins-1 and -2 during nephrogenesis and in autosomal dominant polycystic kidney disease. *Am J Physiol* 1996;271(1 Pt 2):F169-F183.
- Yamamoto T, Sasaki S. Aquaporins in the kidney: emerging new aspects. *Kidney Int* 1998;54:1041-1051.
- Banzi M, Aguiari G, Trimi V, Mangolini A, Pinton P, Witzgall R, *et al.* Polycystin-1 promotes PKCalpha-mediated NF-kappaB activation in kidney cells. *Biochem Biophys Res Commun* 2006;350:257-262.